Desalination and Water Treatment
www.deswater.com

doi: 10.1080/19443994.2015.1131632

57 (2016) 21881–21892
October

Taylor & Francis
Taylor & Francis Group

Zinc and nickel adsorption onto a low-cost mineral adsorbent: kinetic, isotherm, and thermodynamic studies

Arman Emami, Ahmad Rahbar-Kelishami*

Faculty of Chemical Engineering, Iran University Of Science & Technology (IUST), Narmak, Tehran, Iran, Tel. +98 21 77451505; Fax: +982177240495; emails: ar_emami@chemeng.iust.as.ir (A. Emami), ahmadrahbar@iust.ac.ir (A. Rahbar-Kelishami)

Received 12 May 2015; Accepted 1 December 2015

ABSTRACT

In this study, adsorption of zinc and nickel ions from aqueous solutions by low-cost dolomite was investigated. Dolomite, as a mineral adsorbent, is ample in most countries of the world. Morphology of adsorbent surface and the nature of the dolomite powder were examined using the scanning electron microscope. The process has been studied as a function of contact time, pH, initial concentrations, temperature, and adsorbent dosage. The experimental data were evaluated using three isotherm and kinetic models, including the pseudo-first-order, pseudo-second-order, and intraparticle diffusion models for kinetics and Freundlich, Langmuir and Temkin for isotherms. The results showed that the adsorption isotherm data were fitted well by the Langmuir isotherm and adsorption kinetics followed the pseudo-second-order model for both metal ions. The thermodynamic parameters, such as the change in standard free energy, enthalpy, and entropy, were also determined. The calculated parameters indicated that adsorption process was spontaneous and endothermic in nature. The adsorption capacity of zinc and nickel onto dolomite powder found to be 21.85 and 20.09 mg/g, respectively.

Keywords: Zinc; Nickel; Adsorption; Isotherm; Kinetics; Thermodynamics

1. Introduction

Heavy metals, such as Ni(II) and Zn(II) ions, are necessary for animals and plants. However, if these metals are more than the allowed amounts, they will have high toxic effects for living organisms [1,2]. These are persistent and stable environmental contaminants because they are accumulative and non-biodegradable [3]. Zinc and nickel are released into the aquatic environment through several industrial activities, such as metal plating, batteries manufacturing, mining, painting, agricultural sources, and pharmaceutical [4,5]. Therefore, it is necessary to remove Ni(II) and Zn(II) and other harmful metals from aqueous substrates [6].

The common methods for removal of heavy metals from wastewater are chemical precipitation [7], ultrafiltration [8], membrane process [9], biological process [10], ion exchange [11], electrochemical treatment [12], solvent extraction [13], and adsorption [14–16]. However, these methods are limited in comparison with adsorption, due to high operating costs, high rate, high capacity, capability of adsorbent recovery, and ineffective means of resulting sludge disposal. One of disadvantages of adsorption is that for some solutions, some special adsorbents should be used and the

*Corresponding author.

synthesis of these adsorbents is expensive and difficult. Some solutions need adsorbents with very active sites. Also adsorption is not selective [17].

Various adsorbents have been applied for Zn(II), Ni(II), and other metals' removal from industrial effluents, for example, activated carbon, dolomite, zeolite, sawdust, *Spirodela polyrhiza*, and coconut dregs residue [3,6,18–23]. The process cost is an important subject; therefore, the total cost of the process can be reduced using low cost and efficient sorbents.

In recent decades, dolomite has received more attention as an attractive adsorbent. It is a low-cost adsorbent available in many countries such as Iran, China, and India. This is a source of magnesium and calcium. It has a crystal structure, consists of alternative layers of magnesium and calcium carbonate and has a density of about 0.47 cm^3/g. The general formula of this group is $AB(CO_3)_2$ where A can be Ca, Ba, and Sr and B can be Fe, Mg, Zn, and Mn [9,12,13,24]. In this study, the use of powdered dolomite as an adsorbent was experimentally investigated for Zn(II) and Ni(II) removal from aqueous solution. The effects of contact time, pH, initial Zn(II) and Ni(II) concentration, adsorbent dosage and temperature on the adsorption were investigated. Kinetics, isotherms, and thermodynamic studies related to the process were also applied.

2. Experimental

2.1. Materials

2.1.1. Dolomite

Dolomite $CaMg(CO_3)_2$ is very cheap, ample, and accessible around the world. It is worth mentioning that total production cost of dolomite is 8$ per ton approximately [25]. The dolomite was ground and sieved on series of sieves and then it was used as adsorbent for the experiments without any modification like chemical or thermal treatment. The compounds of dolomite used in this work were investigated by X-ray fluorescence (XRF) and are summarized in Table 1.

Table 1
The main chemical compositions of dolomite

Compounds	Weight percent (%)
CaO	31.77
MgO	20.19
SiO_2	0.57
AL_2O_3	0.23
Na_2O	0.06
P_2O_5	0.043
K_2O	0.03
Fe_2O_3	0.01
L.O.I	46.96

2.2. Instrumentation

2.2.1. X-ray diffraction

X-ray diffraction (XRD) relies on the dual wave/particle nature of X-rays to obtain information about the structure of crystalline materials. A primary use of the technique is the identification and characterization of compounds based on their diffraction pattern. The dominant effect that occurs when an incident beam of monochromatic X-rays interacts with a target material is scattering of those X-rays from atoms within the target material. In materials with regular structure (i.e. crystalline), the scattered X-rays undergo constructive and destructive interference. This is the process of diffraction.

2.2.2. Scanning electron microscope

Scanning electron microscopy (SEM) is a method for high-resolution imaging of surfaces. The SEM uses electrons for imaging. Qualitative and quantitative chemical analysis information is also obtained using an energy dispersive X-ray spectrometer (EDS) with the SEM. To create an SEM image, the incident electron beam is scanned in a raster pattern across the sample's surface. The emitted electrons are detected for each position in the scanned area by an electron detector. The intensity of the emitted electron signal is displayed as brightness on a display monitor and/or in a digital image file. By synchronizing the position in the image scan to that of the scan of the incident electron beam, the display represents the morphology of the sample surface area. Magnification of the image is the ratio of the image display size to the sample area scanned by the electron beam.

2.2.3. Fourier transform infrared spectrophotometer

Fourier transform infrared spectroscopy (FTIR) is an analytical technique used to identify organic and inorganic materials. This technique measures the absorption of infrared radiation by the sample material vs. wavelength. The infrared absorption bands identify molecular components and structures.

2.2.4. pH meter

A pH meter is an electronic device used for measuring the pH which is either the concentration of

hydrogen ions in an aqueous solution or the activity of the hydrogen ions in an aqueous solution. The pH will indicate whether the solution is acidic or basic, but is not a measure of acidity or alkalinity. pH meters work in liquids though special probes are sometimes used to measure the pH of semi-solid substances. A typical pH meter consists of a special measuring probe (a glass electrode) connected to an electronic meter that measures and displays the pH reading.

2.2.5. Inductively coupled plasma optical emission spectrometry

Inductively coupled plasma optical emission spectrometry (ICP-OES) is an analytical technique used for the detection of trace metals. It is a type of emission spectroscopy that uses the inductively coupled plasma to produce excited atoms and ions that emit electromagnetic radiation at wavelengths characteristic of a particular element. The intensity of this emission is indicative of the concentration of the element within the sample.

2.2.6. Thermostated shaker

In this study, incubator shaker was used for mixing solution. This shaker has the ability of adjusting the temperature carefully during mixing and can adjust the desired temperature.

2.3. Determination of the zero point charge

The zero point charge of dolomite was determined using the salt addition method in 0.01 M NaCl solutions. A series of mixture of solutions containing 0.1 g adsorbent and 50 ml electrolyte in 250 ml Erlenmeyer flasks were prepared. Initial pH was adjusted in the range of 2–6 and shaken for 48 h. Then, the suspensions were filtered and final pH of the filtrates adsorbent was measured.

2.4. Batch adsorption experiments

$Zn(NO_3)_2{\cdot}4H_2O$ and $Ni(NO_3)_2{\cdot}6H_2O$ (Merck) were prepared by dissolving specified amounts of these materials in double distilled water. Adsorption of zinc and nickel ions was studied as a function of contact time, pH, initial concentrations of zinc and nickel, dosage of adsorbent and temperature in a batch system. The experiments were carried out in different Erlenmeyer flasks with 2 g/L adsorbent on a rotary shaker at 180 rpm at room temperature and centrifuged at 6,000 rpm for 15 min. The contact time effect on adsorption of zinc and nickel was done by adding 1 g of adsorbent in 500 mL of $Zn(NO_3)_2{\cdot}4H_2O$ and $Ni(NO_3)_2{\cdot}6H_2O$ (20 mg L^{-1}) at the temperature 25℃ + 0.1 for several time periods till adsorption reached the equilibrium at 4 h. The effect of pH on the zinc sorption was studied in the range of 2–7. The pH was adjusted with 0.1 M NaOH (98%, Merck) or 0.1 M HCl (Merck). Evaluating the effect of initial concentration of zinc and nickel was performed by applying different concentrations of Ni(II) and Zn(II) in the range of 10–100 ppm. Different temperatures in the range of 25–65℃ for 80 mg/L $Zn(NO_3)_2{\cdot}4H_2O$ and $Ni(NO_3)_2{\cdot}6H_2O$ were applied for studying temperature effect. Experimental results were reported according to the average of a couple of experiments. The zinc and nickel concentrations in the solutions were determined by ICP-OES. Then, the amounts of Zn(II) and Ni(II) adsorbed per unit mass of adsorbent q_t (mg/g) at any time t (min) were calculated by the differences between the final and initial Zn(II) and Ni(II) concentrations in solutions from the following equation:

$$q_t = (C_0 - C_t)\frac{V}{M} \tag{1}$$

where C_t and C_0 (mg L^{-1}) are initial and final concentrations of Zn(II) and Ni(II) in solution, V (L) is the volume of solution, M (g) is the adsorbent weight used in this study. The removal percentage (R, %) of Zn(II) and Ni(II) was calculated by the following equation:

$$R\,(\%) = \frac{C_0 - C_t}{C_0} \times 100 \tag{2}$$

Similar to Eq. (1), C_t and C_0 (mg L^{-1}) are initial and final concentration of Zn(II) and Ni(II) solutions.

2.5. Error analysis

The nonlinear regression has been an important tool to determine the best isotherm model compared to the experimental data. Three nonlinear error functions were applied to evaluate the best fit into the isotherm models to the experimental equilibrium data. The error equations employed were as follows:

Nonlinear chi-square test (χ^2):

$$\chi^2 = \sum_{i=1}^{n}\left[\frac{\left(q_{e,exp} - q_{e,calc}\right)^2}{q_{e,calc}}\right]_i \tag{3}$$

The sum of the squares of the errors (SSE):

$$\mathrm{SSE} = \sum_{i=1}^{N} (q_{\mathrm{e,exp}} - q_{\mathrm{e,calc}})_i^2 \quad (4)$$

Residual root-mean-square error (RMSE):

$$\mathrm{RMSE} = \sqrt{\frac{1}{N-2}\sum_{i=1}^{N} (q_{\mathrm{e,exp}} - q_{\mathrm{e,calc}})^2} \quad (5)$$

In the above equations, the subscripts "exp" and "calc" indicate the experimental and calculated values of adsorption capacities, respectively, and N is the number of observations in the experimental data.

3. Results and discussion

3.1. Characterization of adsorbent

XRD of dolomite powder is presented in Fig. 1. This figure showed that the dolomite has crystal structure consisting dolomite ($CaMg(CO_3)_2$), calcium carbonate ($CaCO_3$), MgO, and SiO_2.

Fig. 2 shows the SEM micrographs of dolomite. As it can be observed in this figure, dolomite is of a rough and irregular surface. Also, its surface is very porous which provides suitable binding site for Ni(II) and Zn(II).

The Fourier transform infrared spectroscopy (FTIR) technique is an important tool to distinguish functional groups, which enables metal adsorption. FTIR spectra of dolomite are shown in Fig. 3.

This figure shows that main peaks of dolomite were formed at 2,524, 1,436, 879, and 727 cm^{-1}. Weak peaks which appeared at 1,040, 799, 522 cm^{-1} indicate the presence of SiO_2 vibrations at silicate phase [26]. The peak at 3,716 cm^{-1} was assigned to hydroxyl group which was joined to Mg and Ca ions.

The surface area and total pore volume of the dolomite are calculated by the standard Brunauer–Emmett–Teller (BET) method. Relative pressure range (P/P_0) for this method was considered between 0.0268 and 0.957. The average pore diameter, specific surface area, and total pore volume were 0.698 nm, 8.907 m^2/g, and 0.472 cm^3/g, respectively.

3.2. Removal of Zn(II) and Ni(II)

3.2.1. Effect of contact time

Contact time is one of the important and effective factors in the adsorption process. The effect of contact

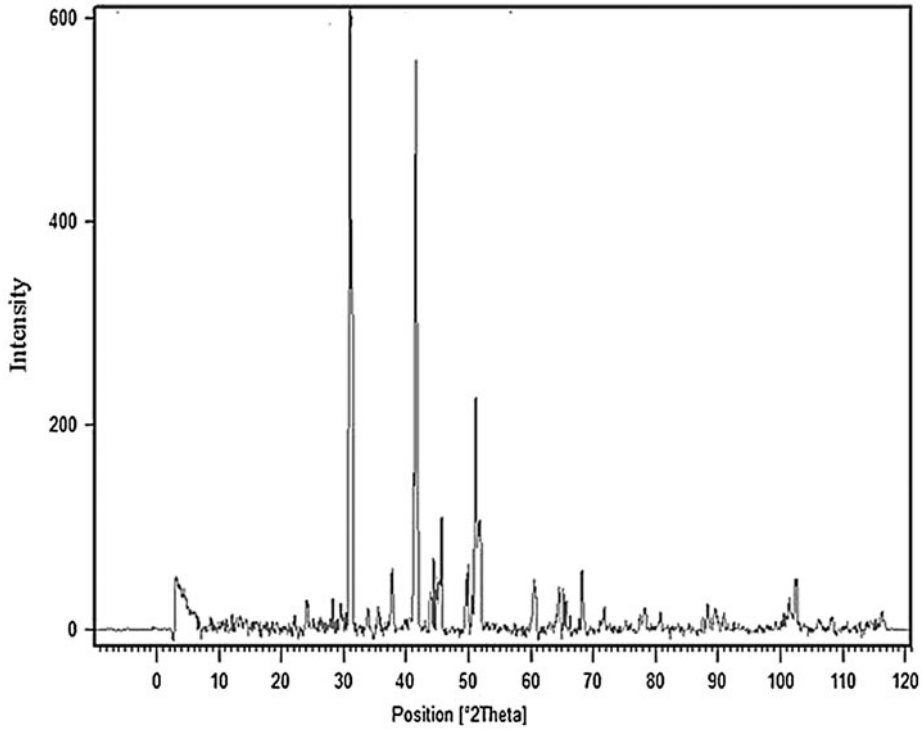

Fig. 1. XRD pattern of dolomite.

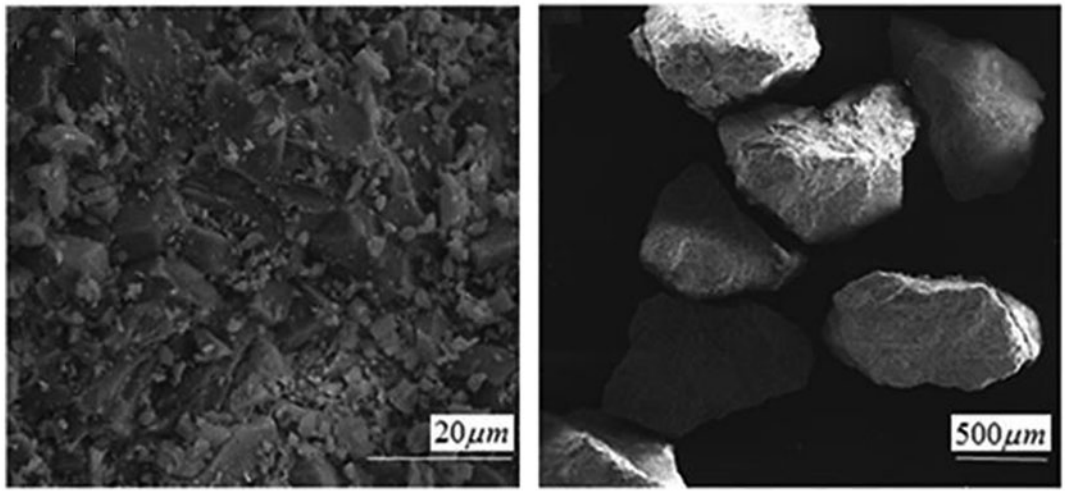

Fig. 2. SEM micrograph of the dolomite.

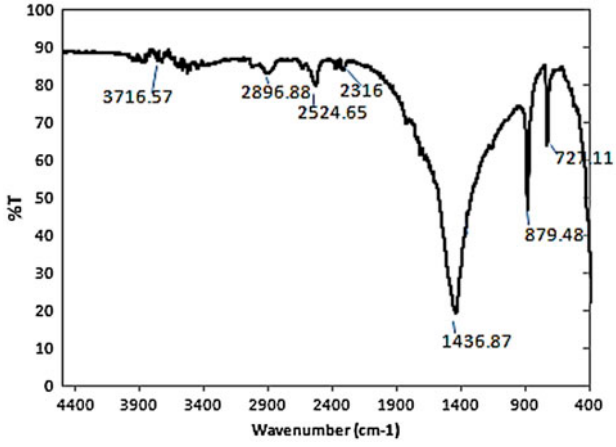

Fig. 3. FTIR spectrum of dolomite.

time for Zn(II) and Ni(II) adsorption onto dolomite is shown in Fig. 4(a). As it is seen, adsorption rate is high in the first 30 and 20 min for Zn(II) and Ni(II), respectively. After this time, the rate decreased slowly and finally equilibrium of adsorption was reached after 150 and 120 min for Zn(II) and Ni(II), respectively. The adsorption process involves two periods: an initial period or fast step and second period or slow step. Equilibrium is made in second period. High rapid rate of adsorption in first step is due to the number of vacant available sites on dolomite surface, and when they are reduced, rate of adsorption decreases until equilibrium occurres [27]. Moreover, decreasing in adsorption rate may occur because of monolayer formation of both metals on the dolomite surface [28].

3.2.2. Effect of pH

Effect of pH on these metals adsorption is presented in Fig. 4(b). With respect to experiments, participation was seen at pH > 7 for both metals. This was why the pH range 2–7 was selected. This figure shows that pH of solution significantly increases adsorption amount. The optimum pH is seen about 5.5 for both metals because the solution pH influences metal speciation and changes charge in the adsorbent (1), and increasing in this significance is due to the density reduction in positive charge at sites on the dolomite and reduction of electrostatic repulsion (2). The solution pH is considerably effective on degree of ionization, metal chemistry and properties of mineral surface, and affects on metal participation. Also operation of functional groups in adsorbent is influenced by this factor [29]. The effect of pH on the zinc and nickel adsorption can be also explained by the calculation of pHzpc value which is presented in Fig. 4(c) and obtained almost 3.5 for dolomite. At pH values lower than pHzpc, the adsorbent surface is positive. There is an electrostatic repulsion between positive charge adsorbent surface and these metal ions, which result in the lower sorption. When pH value is equal to pHzpc, the surface charge of adsorbent is neutral. At pH values greater than pHzpc, the adsorbent surface becomes negatively charged; it causes more attraction of the zinc and nickel ions onto the surface adsorbent and increases the adsorption capacity. At pH values greater than 5.5, the formation of hydroxylated complexes of the zinc and nickel ions in the form of $Zn(OH)_2$ and $Ni(OH)_2$ decreases the adsorption capacity of dolomite [25]. Therefore, the optimum pH for

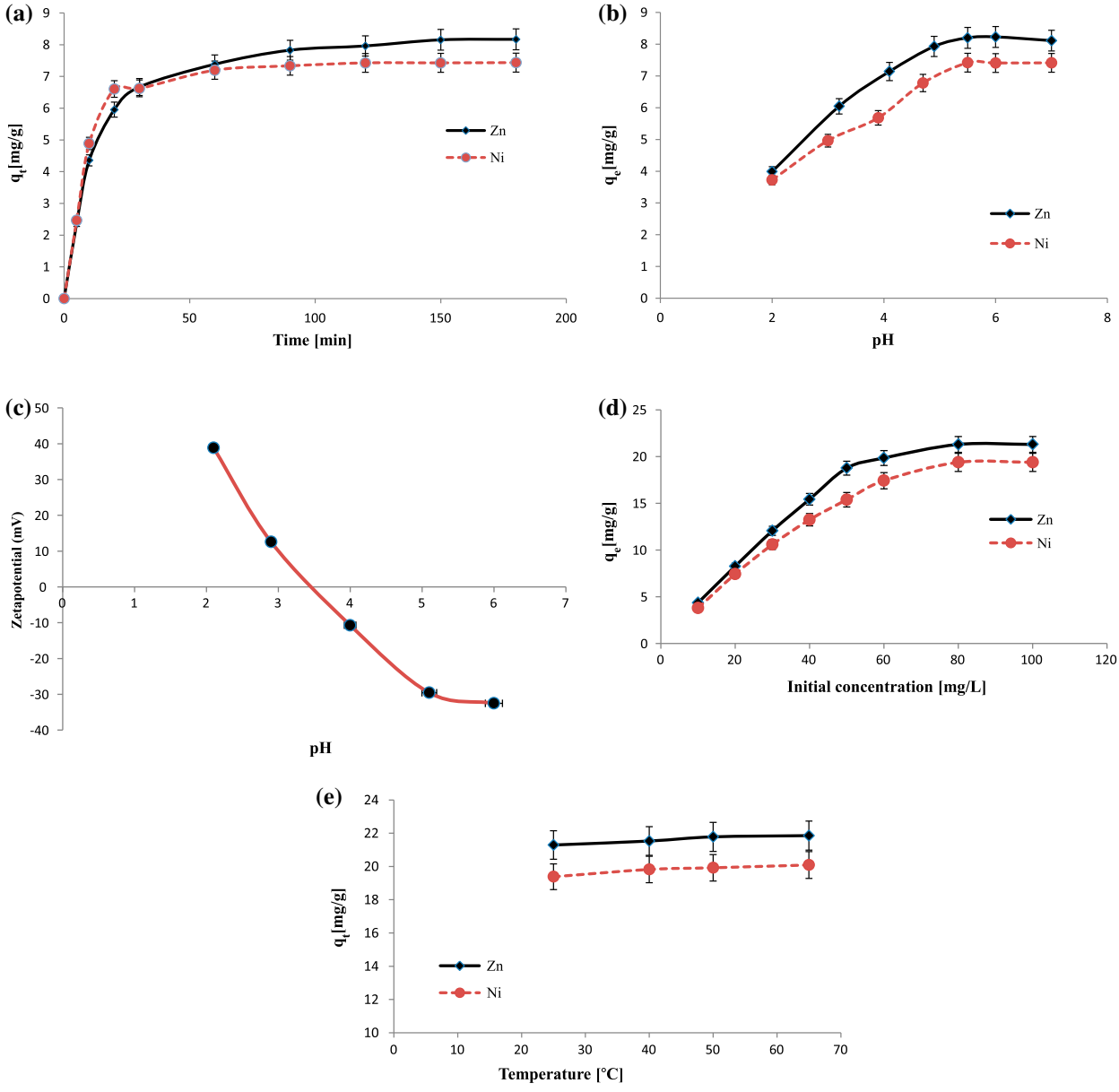

Fig. 4. Effect of parameters on Ni(II) and Zn(II) adsorption: (a) contact time (feed pH of 6, initial Ni(II) and Zn(II) concentration of 20 mg/L, temperature of 25˚C), (b) pH (contact time of 180 min, initial Ni(II) and Zn(II) concentration of 20 mg/L, temperature of 25˚C), (c) the variation of the zeta potential with pH, (d) initial concentration (feed pH of 5.5, contact time of 180 min, temperature of 25˚C), (e) temperature (feed pH of 5.5, initial Ni(II) and Zn(II) concentration of 80 mg/L, contact time of 180 min), (f) effect of adsorbent dosage (feed pH of 5.5, initial Ni(II) and Zn(II) concentration of 20 mg/L, contact time of 180 min, temperature of 25˚C).

further adsorption studies is selected as 5.5 for both metal ions.

3.2.3. Effect of initial concentration

The effect of the initial Zn(II) and Ni(II) concentration on adsorption is shown in Fig. 4(d). It was found that q_e increased with increasing the initial concentrations of Zn(II) and Ni(II). Mass transfer driving force increases and higher adsorption of Zn(II) and Ni(II) occurres [30]. Although after the certain concentration, q_e is not increased because when initial concentration is increased, each unit mass of dolomite is exposed to the large number of metal cations and adsorption sites gradually fill and saturation is obtained [29]. In this

study, optimum concentration was achieved 70 mg/L for Zn and 80 mg/L for Ni.

3.2.4. Effect of temperature

The effect of the temperature on adsorption of Zn (II) and Ni(II) is shown in Fig. 4(e). The experiments were carried out at different temperatures. In most experiments, raising the temperature increased the rate of adsorption. This was due to higher affinity of adsorbent for the cations or increasing the number of active sites on the mineral surface [31]. In some other experiments, sorption capacity was decreased by raising the temperature. It was said that the solubility of metal ions in aqueous medium got better by raising the temperature and it resulted in decreasing in metals concentration on adsorbent surface and the movement of metals to solution phase and as a result, desorption occurred [32].

According to Fig. 4(e), the adsorption capacity is increased by raising the temperature slightly for both metal ions. The results show that adsorption processes of Zn(II) and Ni(II) onto dolomite are endothermic.

3.2.5. Effect of adsorbent dosage

The adsorbent concentration in the solution also influences the adsorption process, since it determines the accessibility of active sites. The increase in the adsorbent concentration causes more sites being available in the same solution volume. It also results in higher adsorption percentage but the value of metal adsorbed per unit adsorbent mass decreases [29]. Effect of this parameter was shown in Fig. 4(f). This figure is plotted adsorption percent against adsorption dosage. With respect to this figure, 5 and 6 g/L dolomite is used for achieving over 98% adsorption for 20 mg/L solution of zinc and nickel.

3.3. Adsorption kinetics

In these experiments, the pseudo-first-order, pseudo-second-order, and intraparticle diffusion models were applied for adsorption kinetics.

Lagergren equation is used for describing adsorption of an adsorbate from an aqueous solution [33]. The liner form of the pseudo-first-order rate model is introduced as follows [23]:

$$\log(q_e - q_t) = \log q_e - \frac{k_1}{2.303}t \quad (6)$$

where q_t and q_e (mg g^{-1}) are values of Zn(II) and Ni (II) adsorbed at time t (min) and equilibrium, k_1 (min^{-1}) is rate constant of Lagergren pseudo-first order. As shown in Fig. 5(a), diagram of $\ln(q_e - q_t)$ vs. t was plotted. Regarding to this plot, k_1 and q_e were obtained by the intercept and the slope, respectively.

The pseudo-second-order rate model is introduced by the following equation [23]:

$$\frac{t}{q_t} = \frac{1}{k_2 q_e^2} + \frac{t}{q_e} \quad (7)$$

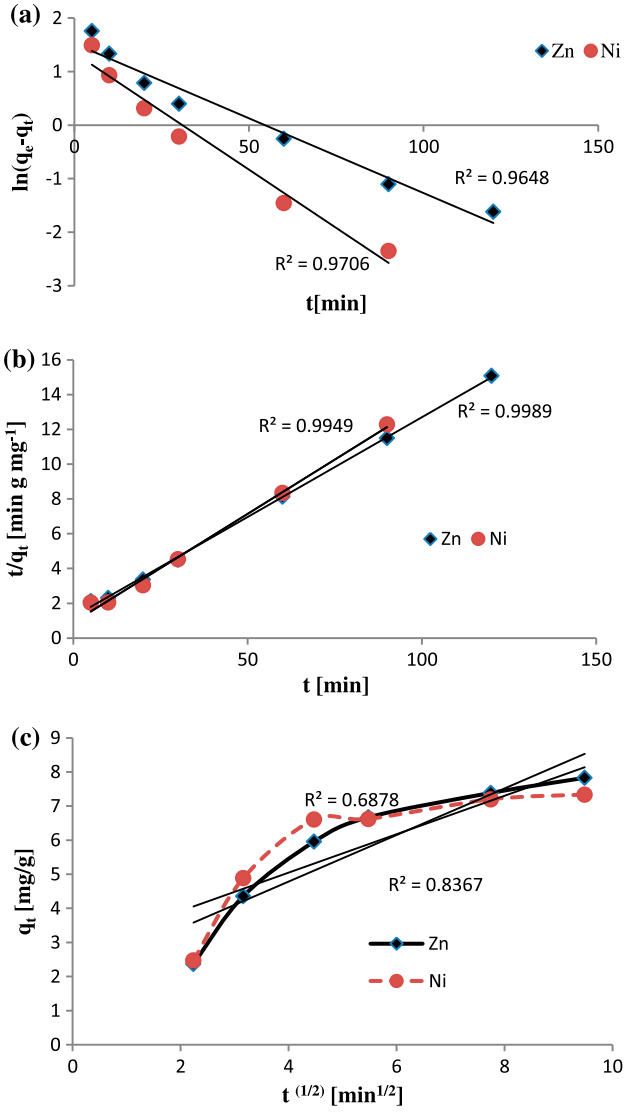

Fig. 5. Adsorption kinetics of Ni(II) and Zn(II) adsorbed by dolomite: (a) pseudo-first-order model, (b) pseudo-second-order model, and (c) intraparticle diffusion model.

Table 2
Adsorption kinetic parameters for Ni(II) and Zn(II) onto the dolomite

	Experiment	Pseudo-first-order			Pseudo-second-order			Intraparticle model		
Metal ion	$q_{e,exp}$ (mg g^{-1})	K_1 (min^{-1})	$q_{e,1cal}$ (mg g^{-1})	R^2	K_2 (g mg^{-1} min^{-1})	$q_{e,2cal}$ (mg g^{-1})	R^2	K_{id} (mg g^{-1} min^{-1})	C (mg/g)	R^2
Zn(II)	8.17	0.028	4.592	0.9648	0.0109	8.711	0.9989	0.683	2.051	0.8367
Ni(II)	7.413	0.044	3.856	0.9706	0.0173	8.013	0.9949	0.563	2.797	0.6878

where q_t and q_e (mg g^{-1}) are similar to equation (4) and k_2 (min^{-1}) is the rate constant of pseudo-second order. As observed in Fig. 5(b) diagram of t/q_t vs. t was plotted. With respect to this plot, k_2 and q_e were determined by the intercept and the slope, respectively.

Intraparticle diffusion is a transport process involving movement of species from the solution bulk to the solid phase. In a well stirred batch adsorption system, the intraparticle diffusion model is used to describe the adsorption process occurring on a porous adsorbent. A plot of the amount of sorbate adsorbed, q_t (mg g^{-1}) and the square root of the time, gives the rate constant by calculating the plot slope. This model can be described by the following equation [34]:

$$q_t = k_{id} t^{1/2} + C_i \tag{8}$$

where k_d (mg/g/$min^{0.5}$) and C_i are diffusion coefficient and intraparticle diffusion constant, respectively. C_i is directly proportional to the thickness of the boundary layer [34]. As observed in Fig. 5(b), diagram of t/q_t vs. t was plotted. With respect to this plot, k_2 and q_e were determined by the intercept and the slope, respectively. For intraparticle diffusion, as shown in Fig. 5(c), diagram of q_t vs. t was plotted, and according to this plot, C and k_{id} were obtained by the intercept and the slope, respectively.

Kinetics parameters of these equations are summarized in Table 2. Regarding Table 2, both Zn(II) and Ni(II) were described by pseudo-second-order rate model. The values of $q_{e,2cal}$ were approximately equal to ($q_{e,exp}$). So pseudo-second-order kinetics reasonably described Zn(II) and Ni(II) adsorption on dolomite.

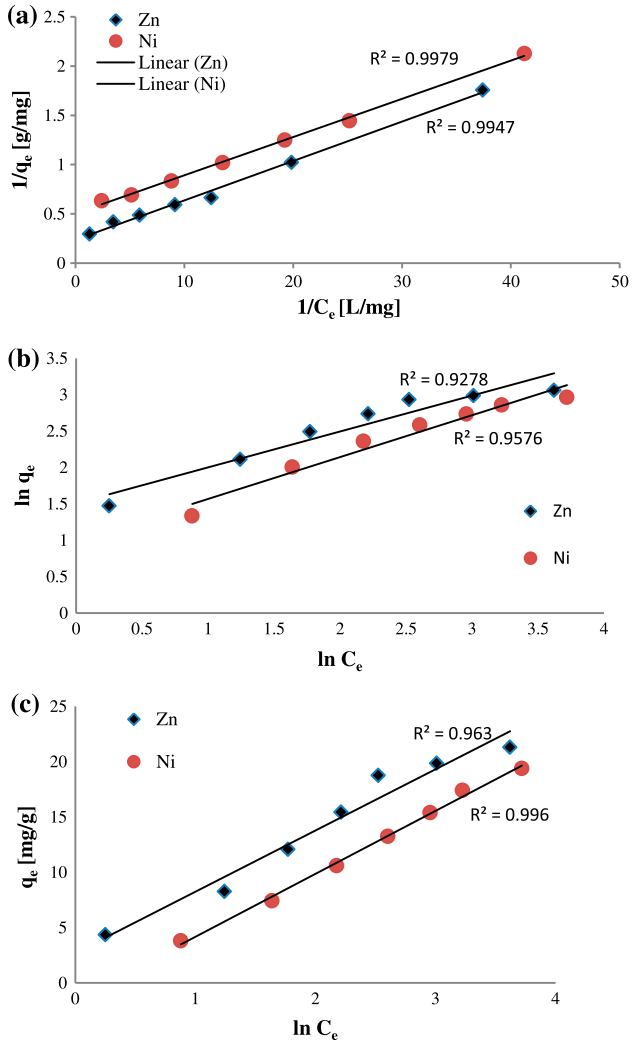

Fig. 6. Adsorption isotherms of Ni(II) and Zn(II) adsorbed by dolomite: (a) Langmuir isotherm model, (b) Freundlich isotherm model, and (c) Temkin isotherm model.

3.4. Adsorption isotherms

In this study, the adsorption parameters were examined using three isotherm models. They were Freundlich, Langmuir, and Temkin.

The Langmuir isotherm model for adsorption is defined as follows [29]:

$$\frac{1}{q_e} = \frac{1}{q_m} + \frac{1}{K_L q_m C_e} \tag{9}$$

where q_e (mg g^{-1}) and C_e (mg L^{-1}) are values of adsorbed metal and metal concentration in

Table 3
Adsorption isotherm parameters for Ni(II) and Zn(II) onto the dolomite

Langmuir						
	q_m (mg/g)	K_L (L/mg)	R^2	χ^2	SSE	RMSE
Zn(II)	25	0.168	0.9947	0.3285	4.7901	0.9787
Ni(II)	23.123	0.0859	0.9979	0.4449	6.5392	1.1436
Freundlich						
	K_F (mg/g) (L/mg)$^{1/n}$	n	R^2	χ^2	SSE	RMSE
Zn(II)	4.0157	1.725	0.9754	4.7147	14.568	5.3957
Ni(II)	2.696	1.739	0.9576	0.9624	16.161	1.7978
Temkin						
	b_T (J/mol)	K_T (L/g)	R^2	χ^2	SSE	RMSE
Zn(II)	448.07	1.636	0.963	0.6314	9.3644	1.3685
Ni(II)	434.85	1.31	0.9801	4.3557	56.657	3.3662

equilibrium state on the adsorbent, q_m (mg g^{-1}) is maximum adsorption capacity, K_L is adsorption energy which is named equilibrium constant or Langmuir constant. This isotherm is supposing monolayer sorption onto a surface with a finite number of identical sites. According to the plot of $1/q_e$ against $1/C_e$ (Fig. 6(a)), the values of q_m and K_L were calculated by the slopes and intercepts. Also, R_L, the dimensionless equilibrium parameter or the separation factor, was determined by Langmuir equation. This equation is as follows [35]:

$$R_L = \frac{1}{1 + K_L C_0} \tag{10}$$

$0 < R_L < 1$ means favorable adsorption while $R_L > 1$, $R_L = 1$, and $R_L = 0$ are, respectively, concerned to unfavorable, linear, and irreversible adsorption. With respect to calculations, values of R_L were obtained for both metals. These values were obtained in the ranges of 0.0562–0.373 for Zn and 0.104–0.538 for Ni. These values show that these processes are favorable.

Freundlich adsorption isotherm model on heterogeneous surfaces is written as [4]:

$$\ln q_e = \ln K_F + \frac{1}{n} \ln C_e \tag{11}$$

where q_e (mg g^{-1}) and C_e (mg L^{-1}) are similar to Eq. (7). K_F (((mg/g)/(mg/L)$^{1/n}$)) and n are constants of Freundlich which are calculated by the plot of ln q_e against ln C_e (Fig. 6(b)). n is defined as heterogeneity factor as well. K_F and n are determined by intercept and slope, respectively.

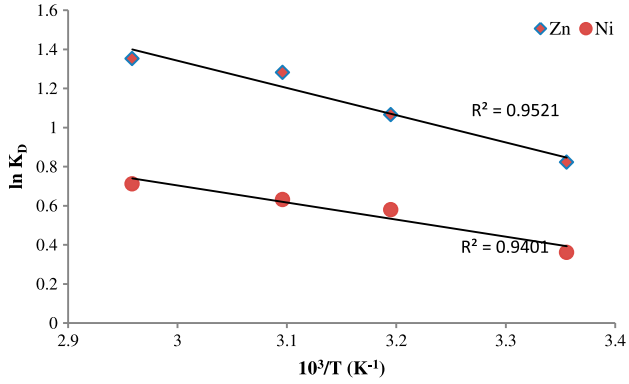

Fig. 7. Van't Hoff plot for the adsorption of Ni(II) and Zn (II) onto the dolomite.

Temkin isotherm model evaluates the enthalpy of adsorption and interactions between adsorbent–adsorbate. Linear form of this equation is shown as [36]:

$$q_e = \frac{RT}{b_T} \ln K_T + \frac{RT}{b_T} \ln C_e \tag{12}$$

where K_T (L/g) is Temkin isotherm equilibrium binding constant, b_T is Temkin isotherm constant concerned to adsorption enthalpy, R is gas universal constant (8.314 J/(mol K)), T is temperature in Kelvin unit. b_T and K_T by are calculated by the slope and the intercept of q_e vs. ln C_e plot (Fig. 6(c)). Parameters of these isotherms are shown in Table 3. As observed, according to values of R^2 obtained from Langmuir, Freundlich, and Temkin isotherms, it is clear that

Table 4
Adsorption thermodynamic parameters for Ni(II) and Zn(II) onto the dolomite

Metal ion	ΔH° (J mol^{-1})	ΔS° (J mol^{-1} K^{-1})	ΔG° (kJ mol^{-1})			
			298	313	323	338
Zn(II)	11.596	45.946	−2.0395	−2.774	−3.444	−3.817
Ni(II)	7.243	27.578	−0.896	−1.509	−1.698	−2.002

Table 5
Comparison of adsorption capacities of various adsorbents for Ni(II) and Zn(II) removal

Adsorbent	q (mg/g) for Zn(II)	q (mg/g) for Ni(II)	Refs.
Melocanna baccifera raw charcoal (MBRC)	4.52	9.53	[6]
Melocanna baccifera activated charcoal (MBAC)	39.32	49.01	[6]
Na-mordenite	–	5.324	[38]
Natural bentonite	47.4	–	[19]
Zeolite 4A	40.38	11.51	[20]
Na-clinoptilolite	14.8	–	[21]
Fly ash	1.301	1.160	[39]
Sawdust	9.57	7.49	
Dye loaded sawdust	17.09	9.87	[40]
Dye loaded groundnut shells	7.62	3.83	
Activated carbon	22.03	17.21	[41]
Dolomite	21.856	20.09	This study

Langmuir isotherm with R^2 equal to 0.9947 for Zinc and 0.9979 for nickel can describe the Ni(II) and Zn(II) adsorption on dolomite very well. In addition, it can be seen in Table 3 that the values of error analyses for the Langmuir for Ni(II) and Zn(II) are lower than that of the other isotherms, which verifies the applicability of the Langmuir isotherm model for adsorption of Ni (II) and Zn(II) onto the dolomite. Adsorption mechanism follows this isotherm that one layer of adsorbate molecules can join on the surface of adsorbent with the same adsorption energy and reversible bondings.

3.5. Adsorption thermodynamics

Thermodynamic parameters can be calculated by making experiments in different temperatures. These parameters are changes in enthalpy (ΔH°), standard free energy (ΔG°), and entropy (ΔS°) which are determined for adsorption of Zn(II) and Ni(II) onto dolomite. Above-mentioned parameters can be calculated using the following equations [37]:

$$K_D = \frac{q_e}{C_e} \tag{13}$$

$$\Delta G^\circ = -RT \ln K_D \tag{14}$$

$$\ln K_D = \frac{\Delta S^\circ}{R} - \frac{\Delta H^\circ}{RT} \tag{15}$$

where K_D is the sorption distribution coefficient. In Eq. (15), ΔH° and ΔS° are determined from slope and intercept of the plot of ln K_D against $1/T$ (Fig. 7). Standard Gibbs free energy change of sorption (ΔG°) was evaluated using Eq. (14).

The calculated thermodynamic parameters are presented in Table 4. The negative Gibbs free energy changes (ΔG°) value and the positive value of ΔH° indicate that the adsorption process is spontaneous and endothermic, respectively. Also the positive value of entropy changes (ΔS°) shows randomness nature of process at the solid/solution interface and the affinity of dolomite for Ni(II) and Zn(II) adsorption [32,37].

3.6. Comparison of various adsorbents

Table 5 compares the adsorption capacities of the dolomite in this work with some various sorbents previously used for Zn(II) and Ni(II) removal. As observed, the adsorption capacities of the dolomite (q_m) are good for using because it is very inexpensive and available. So, dolomite is a suitable sorbent.

4. Conclusion

In this study, dolomite powder appears as a very cheap and available adsorbent for Zn(II) and Ni(II) removal from aqueous solution. The operating parameters for the maximum adsorption of Zn(II) were initial concentration of 70 mg/L, temperature of 343 K, contact time of 150 min, and pH of 5.5. The maximum adsorption of Ni(II) occurred in initial concentration of 80 mg/L, temperature of 343 K, contact time of 120 min, and pH of 5.5. The kinetics of Zn(II) and Ni (II) adsorption on dolomite followed the pseudo-second-order rate model. Equilibrium data were fitted very well by Langmuir isotherm equation. Maximum adsorption capacity was determined 21.856 for zinc and 20.09 mg/g for nickel. The negative ΔG° value indicated that the adsorption was feasible and spontaneous. The positive ΔH° and ΔS° values described endothermic nature of the adsorption and the affinity of dolomite for Zn(II) and Ni(II) adsorption, respectively. Adsorption is chemical forces binding Ni^{2+} and Zn^{2+} ions to the surface of the dolomite.

References

[1] N. Kawasaki, H. Tominaga, F. Ogata, K. Kakehi, Removal of cadmium and copper by vegetable biomass treated with hydrochloric acid, Chem. Eng. J. 157 (2010) 249–253.

[2] Z. Özlem, Y. Yürüm, Synthesis and characterization of anatase nanoadsorbent and application in removal of lead, copper and arsenic from water, Chem. Eng. J. 225 (2013) 625–635.

[3] M.D. Meitei, M.N.V. Prasad, Adsorption of Cu(II), Mn(II) and Zn(II) by *Spirodela polyrhiza* (L.) Schleiden: Equilibrium, kinetic and thermodynamic studies, Ecol. Eng. 71 (2014) 308–317.

[4] A. Olgun, N. Atar, Removal of copper and cobalt from aqueous solution onto waste containing boron impurity, Chem. Eng. J. 167 (2011) 140–147.

[5] O. Abdelwahab, N.K. Amin, E.-S.Z. El-Ashtoukhy, Removal of zinc ions from aqueous solution using a cation exchange resin, Chem. Eng. Res. Des. 91 (2013) 165–173.

[6] H. Lalhruaitluanga, M.N.V. Prasad, K. Radha, Potential of chemically activated and raw charcoals of Melocanna baccifera for removal of Ni(II) and Zn(II) from aqueous solutions, Desalination 271 (2011) 301–308.

[7] Y. Kim, T. Ogata, Y. Nakano, Kinetic analysis of palladium(II) adsorption process on condensed-tannin gel based on redox reaction models, Water Res. 41 (2007) 3043–3050.

[8] E. Samper, M. Rodríguez, M.A. De la Rubia, D. Prats, Removal of metal ions at low concentration by micellar-enhanced ultrafiltration (MEUF) using sodium dodecyl sulfate (SDS) and linear alkylbenzene sulfonate (LAS), Sep. Purif. Technol. 65 (2009) 337–342.

[9] N. Ghaemi, S.S. Madaeni, P. Daraei, H. Rajabi, T. Shojaeimehr, F. Rahimpour, B. Shirvani, PES mixed matrix nanofiltration membrane embedded with polymer wrapped MWCNT: Fabrication and performance optimization in dye removal by RSM, J. Hazard. Mater. 298 (2015) 111–121.

[10] E. Pehlivan, A.M. Özkan, S. Dinç, Ş. Parlayici, Adsorption of Cu^{2+} and Pb^{2+} ion on dolomite powder, J. Hazard. Mater. 167 (2009) 1044–1049.

[11] A. Shafaei, F.Z. Ashtiani, T. Kaghazchi, Equilibrium studies of the sorption of Hg(II) ions onto chitosan, Chem. Eng. J. 133 (2007) 311–316.

[12] A. Ghaemi, M. Torab-Mostaedi, M. Ghannadi-Maragheh, Characterizations of strontium(II) and barium(II) adsorption from aqueous solutions using dolomite powder, J. Hazard. Mater. 190 (2011) 916–921.

[13] A.B. Albadarin, C. Mangwandi, A. Al-Muhtaseb, G.M. Walker, S.J. Allen, M.N.M. Ahmad, Kinetic and thermodynamics of chromium ions adsorption onto low-cost dolomite adsorbent, Chem. Eng. J. 179 (2012) 193–202.

[14] J. Mittal, D. Jhare, H. Vardhan, A. Mittal, Utilization of bottom ash as a low-cost sorbent for the removal and recovery of a toxic halogen containing dye eosin yellow, Desalin. Water Treat. 52 (2014) 4508–4519.

[15] H.Z. Mousavi, S.R. Seyedi, Nettle ash as a low cost adsorbent for the removal of nickel and cadmium from wastewater, Int. J. Environ. Sci. Technol. 8 (2011) 195–202.

[16] M. Peydayesh, A. Rahbar-Kelishami, Adsorption of methylene blue onto *Platanus orientalis* leaf powder: Kinetic, equilibrium and thermodynamic studies, J. Ind. Eng. Chem. 21 (2015) 1014–1019.

[17] X. Tong, R. Xu, Removal of Cu(II) from acidic electroplating effluent by biochars generated from crop straws, J. Environ. Sci. 25 (2013) 652–658.

[18] X.S. Wang, J. Huang, H.Q. Hu, J. Wang, Y. Qin, Determination of kinetic and equilibrium parameters of the batch adsorption of Ni(II) from aqueous solutions by Na-mordenite, J. Hazard. Mater. 142 (2007) 468–476.

[19] T.K. Sen, D. Gomez, Adsorption of zinc (Zn^{2+}) from aqueous solution on natural bentonite, Desalination 267 (2011) 286–294.

[20] K.S. Hui, C.Y.H. Chao, S.C. Kot, Removal of mixed heavy metal ions in wastewater by zeolite 4A and residual products from recycled coal fly ash, J. Hazard. Mater. 127 (2005) 89–101.

[21] D. Stojakovic, J. Hrenovic, M. Mazaj, N. Rajic, On the zinc sorption by the Serbian natural clinoptilolite and the disinfecting ability and phosphate affinity of the exhausted sorbent, J. Hazard. Mater. 185 (2011) 408–415.

[22] L.S. de Lima, S.P. Quináia, F.L. Melquiades, G.E.V. de Biasi, J.R. Garcia, Characterization of activated carbons from different sources and the simultaneous adsorption of Cu, Cr, and Zn from metallurgic effluent, Sep. Purif. Technol. 122 (2014) 421–430.

[23] A. Kamari, S.N.M. Yusoff, F. Abdullah, W.P. Putra, Biosorptive removal of Cu(II), Ni(II) and Pb(II) ions from aqueous solutions using coconut dregs residue: Adsorption and characterisation studies, J. Environ. Chem. Eng. 2 (2014) 1912–1919.

[24] K. Sasaki, M. Yoshida, B. Ahmmad, N. Fukumoto, T. Hirajima, Sorption of fluoride on partially calcined dolomite, Colloids Surf., A: Physicochem. Eng. Aspects 435 (2013) 56–62.

[25] M. Irani, M. Amjadi, M.A. Mousavian, Comparative study of lead sorption onto natural perlite, dolomite and diatomite. Chem. Eng. J. 178 (2011) 317–323.
[26] S. Gunasekaran, G. Anbalagan, Thermal decomposition of natural dolomite, Indian Acad. Sci. 30 (2007) 339–344.
[27] M. Kapur, M.K. Mondal, Competitive sorption of Cu (II) and Ni(II) ions from aqueous solutions: Kinetics, thermodynamics and desorption studies, J. Taiwan Inst. Chem. Eng. 45 (2014) 1083–1094.
[28] D. Pathania, S. Sharma, P. Singh, Removal of methylene blue by adsorption onto activated carbon developed from *Ficus carica* bast. Arab. J. Chem (in press) 1–7, doi: 10.1016/j.arabjc.2013.04.021.
[29] S. Malamis, E. Katsou, A review on zinc and nickel adsorption on natural and modified zeolite, bentonite and vermiculite: Examination of process parameters, kinetics and isotherms, J. Hazard. Mater. 235–252 (2013) 428–461.
[30] X. Han, W. Wang, X. Ma, Adsorption characteristics of methylene blue onto low cost biomass material lotus leaf, Chem. Eng. J. 171 (2011) 1–8.
[31] N. Goyal, S.C. Jain, U.C. Banerjee, Comparative studies on the microbial adsorption of heavy metals, Adv. Environ. Res. 7 (2003) 311–319.
[32] M. Baek, C.O. Ijagbemi, O. Se-Jin, D. Kim, Removal of Malachite Green from aqueous solution using degreased coffee bean, J. Hazard. Mater. 176 (2010) 820.
[33] R.B. Garcia-Reyes, R.R.-M. Jose, Adsorption kinetics of chromium (III) ions on agro-waste materials, Bioresour. Technol. 101 (2010) 8099–8108.
[34] A.U. Itodo, F.W. Abdulrahman, L.G. Hassan, S.A. Maigandi, H.U. Itodo, Intraparticle diffusion and intraparticulate diffusivities of herbicide on derived activated carbon, Researcher 2 (2010) 2.
[35] S. Kocaoba, Comparison of Amberlite IR 120 and dolomite's performances for removal of heavy metals, J. Hazard. Mater. 147 (2007) 488–496.
[36] F. Hemmati, R. Norouzbeigi, F. Sarbisheh, H. Shayesteh, Malachite green removal using modified sphagnum peat moss as a low-cost biosorbent: Kinetic, equilibrium and thermodynamic studies, J. Taiwan Inst. Chem. Eng. (in press) 1–8, doi: 10.1016/j.jtice.2015.07.004.
[37] S.R. Shukla, R.S. Pai, Adsorption of Cu(II), Ni(II) and Zn(II) on dye loaded groundnut shells and sawdust, Sep. Purif. Technol. 43 (2005) 1–8.
[38] X.S. Wang, J. Huang, H.Q. Hu, J. Wang, Y. Qin, Determination of kinetic and equilibrium parameters of the batch adsorption of Ni(II) from aqueous solutions by Na-mordenite, J. Hazard. Mater. 142 (2007) 468–476.
[39] E.F. Covelo, F.A. Vega, M.L. Andrade, Sorption and desorption of Cd, Cr, Cu, Ni, Pb and Zn by a Fibric Histosol and its organo-mineral fraction, J. Hazard. Mater. 159 (2008) 342–347.
[40] S.R. Shukla, R.S. Pai, Adsorption of Cu(II), Ni(II) and Zn(II) on dye loaded groundnut shells and sawdust, Sep. Purif. Technol. 43 (2005) 1–8.
[41] H. Kalavathy, B. Karthik, L.R. Miranda, Removal and recovery of Ni and Zn from aqueous solution using activated carbon from *Hevea brasiliensis*: Batch and column studies, Colloids Surf., B: Biointerfaces 78 (2010) 291–302.